PTEN Inhibition Accelerates Corneal Endothelial Wound Healing through Increased Endothelial Cell Division and Migration

Weijie Zhang,[1,2] Fei Yu,[1,2] Chenxi Yan,[1,2] Chunyi Shao,[1,2] Ping Gu,[1,2] Yao Fu,[1,2] Hao Sun,[1,2] and Xianqun Fan[1,2]

[1]Department of Ophthalmology, Ninth People's Hospital, Shanghai Jiao Tong University, School of Medicine, Shanghai, China
[2]Shanghai Key Laboratory of Orbital Diseases and Ocular Oncology, Shanghai, China

Correspondence: Xianqun Fan, 639 Zhizaoju Road, Shanghai, China; fanxq@sjtu.edu.cn.
Hao Sun, 639 Zhizaoju Road, Shanghai, China; sunhao6666@126.com.
Yao Fu, 639 Zhizaoju Road, Shanghai, China; fuyaofy@sina.com.

WZ and FY contributed equally to this work.

Received: December 30, 2019
Accepted: June 18, 2020
Published: July 15, 2020

Citation: Zhang W, Yu F, Yan C, et al. Pten inhibition accelerates corneal endothelial wound healing through increased endothelial cell division and migration. *Invest Ophthalmol Vis Sci.* 2020;61(8):19. https://doi.org/10.1167/iovs.61.8.19

Purpose. To investigate the role of phosphatase and tensin homologue deleted on chromosome 10 (PTEN) in the regulation of corneal endothelial cell (CECs) focusing on proliferation and migration, and to further evaluate the application of PTEN inhibitors in the treatment of corneal endothelial dysfunction in a rat model.

Methods. Expression of PTEN in human and rat corneal endothelium was determined by immunocytochemistry, western blotting, and ELISA. A small molecular inhibitor of PTEN, bpV(pic), was applied in the culture of human CEC cell line B4G12 and organ-cultured rat cornea in the presence of transforming growth factor beta 2 (TGF-β2). Cell cycle status was detected by flow cytometry and BrdU staining. Subcellular localization for endogenous p27Kip1 was detected by immunocytochemistry and western blotting. Moreover, exogenous transfected YFP-p27Kip1 was observed under a fluorescent microscope. Cell migration was examined with a wound scratch model and transwell invasion assay. Finally, bpV(pic) was intracamerally injected in a rat corneal endothelial injury model. The wound healing process was evaluated by slit lamp biomicroscopy, optical coherence tomography, histological and scanning electron microscope examination.

Results. The expression of PTEN in human corneal endothelium was higher compared with rat, which we speculate was mostly responsible for the relatively less proliferation capacity of human CEC than rat. PTEN inhibition by bpV(pic) could reverse TGF-β2-induced CEC G1-arrest by alleviating p27Kip1 nuclear accumulation and decreasing total p27Kip1 expression. In addition, bpV(pic) promoted CEC migration, which acted synergistically with TGF-β2. Finally, intracameral injection of bpV(pic) could promote corneal endothelial wound healing in a rat model.

Conclusions. Our study provided experimental basis for the development of therapeutic agent targeting on PTEN for the treatment of corneal endothelial dysfunction.

Keywords: corneal endothelial cells, cell cycle, migration, PTEN

Corneal endothelial dysfunction is a common sight-threatening condition for which treatment options are extremely limited. Many etiologies, including aging, trauma, endothelial dystrophy, and systemic disease, lead to corneal endothelial dysfunction. Corneal transplantation is a well-established treatment for corneal endothelial dysfunction. However, the procedure is severely limited by a global shortage of donors and graft failures.[1,2] Consequently, there is an urgent need for the development of new pharmaceutical products for the treatment of corneal endothelial dysfunction, which necessitates further exploration of the underlying molecular mechanisms relating to corneal endothelial cell (CEC) proliferation and migration.

The corneal endothelium lines the innermost layer of the cornea, serving as a barrier between the stroma and the aqueous humor. In addition, the corneal endothelium also acts as a fluid pump to maintain the relatively dehydrated status of corneal stroma. Derived from the neural crest during embryologic development, CEC are arrested in the G1-phase and rarely divide after birth.[3,4] Researchers have proposed that the high concentration of transforming growth factor beta 2 (TGF-β2) in aqueous humor and cell-cell contact-dependent inhibition (once compact monolayer of corneal endothelium is formed) are two main causes of G1-arrest status of CEC.[5–7] In addition, lack of effective growth factors, such as basic fibroblast growth factor, insulin-like growth factor-I and -II (IGF-1 and IGF-2), hepatocyte growth factor, and others, in the aqueous humor might also contribute to the limited proliferation capacity of CEC in vivo.

Several species-specific characteristics have been observed in the proliferative capacity of CECs. When injured by trauma, aging, inflammation, or other etiologies, the wound healing process of primates and feline corneal

endothelium occurs by cell migration and enlargement of adjacent healthy CECs, rather than by cell proliferation. In contrast, CECs from rats and rabbits are released from G1-arrest, and initiate the wound healing process through cell division and migration.[8–10] Moreover, CECs from bovine, rabbits, and rats have relatively high proliferation capacity when cultured in vitro, whereas CECs from feline and primates are difficult to amplify.[11–13] The differential mechanism controlling CEC proliferation and sensitivity to TGF-β2-induced G1-arrest across different species remains to be elucidated. Further studies focusing on resolving interspecies differences may lead to the development of novel therapies to promote human CEC proliferation.

Phosphatase and tensin homologue deleted on chromosome 10 (PTEN) is located on chromosome 10q23.3. The gene encodes the PTEN protein, which acts to downregulate the phosphoinositide 3-kinases (PI3Ks)/Akt signaling pathway and as a tumor suppressor by regulating cell cycle progression, apoptosis, and migration.[14–16] Studies have proved that the expression level of PTEN was related to cell cycle progression of tumor cells[17] and normal cells.[18] Moreover, Akt activation was found to be related to tumor malignancy by contributing to resistance to TGF-β2-induced G1-arrest. Therefore we speculated whether PTEN played a role in the CEC cell cycle arrest status induced by TGF-β2. Meanwhile, in corneal epithelial cells, PTEN was found to regulate cell migration during wound healing.[19,20] Taken together, a hypothesis is built that PTEN might participate in the corneal endothelial wound healing process by mediating cell cycle progression and migration.

In this study, we found that differential expression of PTEN in the corneal endothelium of humans and rats may cause interspecies differences in cell cycle status and proliferation capacity. PTEN inhibition released human CECs from G1-arrest status and increased cell migration in the presence of TGF-β2, by facilitating the nuclear export of p27Kip1 and activation of the Akt pathway. Moreover, intracameral injection of PTEN inhibitors could promote wound healing in rat corneal endothelial injury models.

Materials and Methods

Plasmids, Drugs, and Antibodies

YFP-p27Kip1 plasmid was transiently transfected into B4G12 using Lipofectamine 2000 (Thermo Fisher Scientific, Waltham, MA, USA) according to the manufacturer's instructions.

Before the experiment proper starts, we carried out a series of preliminary experiments to determine the appropriate drug dosage (see Supplementary Fig. S1). The PTEN inhibitor, bpv(pic) (Sigma-Aldrich, St. Louis, MO, USA) was used at a final concentration of 1 µM for the organ culture of the rat cornea and at 10 µM for the culture of B4G12. The PI3K/Akt inhibitor, LY294002 (Sigma-Aldrich), was used at a final concentration of 10 µM. Human recombinant TGF-β2 (Cell Signaling Technology, Danvers, MA, USA) was used at a final concentration of 10 ng/mL.

The following primary antibodies and dilutions were used: mouse Anti-GAPDH (Thermo Fisher Scientific, 1:5000 for western blotting), rabbit Anti-ZO-1 (Santa Cruz Biotechnology, Santa Cruz, CA, USA, 1:200 for immunofluorescence, 1:50 for immunohistochemistry), mouse Anti-BrdU (Abcam, Cambridge, MA, USA, 1:200 for immunofluorescence, 1:100 for immunohistochemistry), rabbit anti-PTEN (Cell Signaling Technology, 1:100 for immunofluorescence, 1:1000 for western blotting), rabbit Anti-p27Kip1 (Cell Signaling Technology, 1:100 for immunofluorescence, 1:1000 for western blotting), and Alexa Fluor 488 Phalloidin (Thermo Fisher Scientific, 5 units/mL for immunofluorescence).

Donor Tissues and Ethical Review

Human corneoscleral rims derived from the donor corneas for transplantation were obtained from the department of ophthalmology, Ninth People's Hospital affiliated to Shanghai Jiao Tong University School of Medicine. All subjects were treated in accordance with the Declaration of Helsinki. The procedure was approved by the ethics committee of Shanghai Ninth People's Hospital.

SPF Sprague Dawley rats aged 8 weeks were obtained from the Shanghai Animal Experimental Center. All animals were treated in accordance with the ARVO Statement for the Use of Animals in Ophthalmic and Vision Research. All procedures were approved by the Animal Research Committee of Ninth People's Hospital, Shanghai Jiao Tong University School of Medicine.

Protein Extraction and Western Blotting

Whole-cell extracts from human and rat corneal endothelium were lysed with precooled RIPA lysis buffer (Millipore, Billerica, MA, USA) in the presence of protease and phosphatase inhibitors (Roche, Mannheim, BW, Germany). After brief sonication, the concentrations of the extracted samples were determined by the BCA assay kit (Thermo Fisher Scientific). A total of 20 to 30 µg of protein were electrophoresed on an SDS-PAGE gel (Bio-Rad Laboratories, Hercules, CA, USA) and immunoblotted with the specified antibodies. GAPDH was used as a loading control. For protein extraction from different fractions of B4G12, the NE-PER nuclear and cytoplasmic extraction reagents (Thermo Fisher Scientific) were used according to the manufacture's protocol. GAPDH and SP1 were respectively used for cytoplasmic and nuclear loading controls.

Enzyme-Linked Immunosorbent Assay (ELISA)

The quantity of PTEN in human and rat corneal endothelium tissues was measured using Human and Rat PTEN ELISA Kits (ELK Biotechnology, Wuhan, China), respectively, according to the manufacturer protocol. Briefly, standards were serially diluted into eight standard diluents, each half of the previous starting from concentrations of 20 ng/mL. A total of 100 µL of blank solution, the standards and samples were added into a 96 well plate and incubated for 2 hours at 37°C. After washing three times, 100 µL of biotinylated antibody working solution and Streptavidin-HRP working solution were added in order into each well and incubated for 1 hour at 37°C, followed by the addition of TMB substrate solution. Finally, the OD at 450 nm was immediately read. The standard curve was constructed by plotting the mean OD and concentration for each standard. Regression analysis was used to calculate the line of best fit to measure PTEN concentrations in rat and human samples.

Cell Culture

The human immortalized CEC line B4G12 was purchased from the Creative Bioarray (Shirley, NY, USA) and cultured

in Dulbecco's Modified Eagle Medium (DMEM) containing 10% fetal bovine serum (FBS) and 50 U/mL penicillin and streptomycin antibiotics.

Flow Cytometry and Immunocytochemistry

Cells were synchronized in the G0/G1 phase after growth in DMEM containing 2% FBS for 24 hours. Synchronized cells were cultured in DMEM containing 5% FBS with or without TGF-β2 and bpV(pic) as indicated for another 24 hours. Then cells were fixed in 75% precooled ethyl alcohol at 4°C overnight. Cells were stained with propidium iodide-RNase solution, and cell cycle analysis was carried out using a CytoFLEX flow cytometry system (Beckman Coulter, Brea, CA, USA).

For BrdU IHC staining, cells were pretreated with 10 µM BrdU at 37°C for 30 minutes, and then fixed with 4% paraformaldehyde (PFA). DNA was hydrolyzed by 2 N HCl (Sigma-Aldrich). IHC was performed using mouse anti-BrdU primary antibody. Images were viewed under a confocal microscope (Nikon Instruments, Tokyo, Japan).

Organ Culture

The cornea organ culture was performed according to established protocols.[21,22] SPF Sprague Dawley eyeballs were surgically removed, and corneas were excised and placed in 24-well culture plates with the endothelium facing upward. Opti-MEM I media (Thermo Fisher Scientific) supplemented with 10 ng/mL TGF-β2 was used as the basal media, with or without 1 µM bpV(pic).

Histology and Immunofluorescence

Human and rat corneas were fixed with 4% PFA and then embedded with an optimal cutting temperature compound for cryosection at 10 µm. After dehydration, sections were stained for immunofluorescence with anti-PTEN antibody as described earlier. F-actin filaments were stained with anti-phalloidin antibody and cell nuclei were counterstained with DAPI. An equal amount of antibody diluent alone (with no PTEN primary antibody), followed by incubation with secondary antibody (Cy3 conjugated anti-rabbit IgG antibody), was used as negative control (see Supplementary Fig. S2).

Migration and Invasion Assay

B4G12 cells were seeded in 24-well culture plates at a cell density of 8×10^4/well and cultured in DMEM supplemented with 10% FBS until a confluent cell monolayer formed. A scratch wound was made in the center of each well with a 200-µL tip as previously described.[20] Culture medium was changed to DMEM containing 5% FBS with or without TGF-β2, LY294002, and bpV(pic) as indicated, and cells cultured for 6 hours. Images were acquired using a bright-field microscope to record cell migration.

For the cell invasion assay, B4G12 cells were suspended in DMEM containing 2% FBS at a cell density of 2×10^6/mL, and 200 µL of cell suspension seeded into a transwell chamber. DMEM containing 5% FBS with or without TGF-β2, LY294002, and bpV(pic) as indicated, was added to the wells. After incubation overnight, the transwell insert was immersed in methyl alcohol at room temperature for 10 minutes, followed by staining with 0.1% Crystal Violet solution (Selleck Chemicals LLC, Houston, USA). The noninvading cells at the top of the inserts were rubbed with a cotton swab, and the invaded cells that had attached to the basal surface were observed under a microscope.

Intracameral Injection of bpV(pic) in a Rat Corneal Endothelial Injury Model

A rat corneal endothelial injury model was established with intracameral injection of 0.05% benzalkonium chloride according to previous studies.[23,24] Specifically, SPF Sprague Dawley rats at 8 weeks old underwent general anesthesia with intraperitoneal injection of 10% chloral hydrate (w/v, 0.3 mL/100g), and were randomly assigned into two groups. The right eyes were operated, and the left eyes were left untreated. After topical application of mydriatic eye drops, a 32-gauge needle was used to puncture the paracentral cornea, and the aqueous humor was allowed to flow out. A total of 5 µL of 0.05% benzalkonium chloride was intracamerally injected and rinsed for 1 minute, followed by rinsing with 0.9% sodium chloride for 2 minutes. In the control group, 5 µL of modified Opti-MEM I medium was injected through the existing puncture point, and a small air bubble was made to seal the corneal puncture. For the bpV(pic) group, 5 µL of modified Opti-MEM I medium containing 10 µM bpV(pic) was injected into the anterior chamber in the same way.

Follow-Up of Corneal Endothelial Wound Healing

Thirty minutes after injection of benzalkonium chloride, and at 7 and 14 days after injection of Opti-MEM I medium or bpV(pic), two rats from each group were sacrificed for scanning electron microscope (SEM) and IHC examinations. At each time point, slit lamp biomicroscopy (Topcon, Inc., Tokyo, Japan) and optical coherence tomography (OCT) (Heidelberg Engineering, Heidelberg, Germany) were applied to examine wound healing in the corneal endothelium.

Corneal edema was graded according to the following classification: 0 = completely transparent cornea; 1 = minimal loss of transparency, with the iris vessels clearly visible; 2 = moderate corneal cloudiness, with the iris vessels partly visible; 3 = severe corneal haze, with only pupil margin visible; and 4 = severe corneal opacification, with the anterior chamber structure completely invisible.

At each time point, four rats from each group were euthanizedand the eyeballs were enucleated. The left eyeballs served as normal controls before the operation. Corneas, including the limbus region, were excised, and divided in half. One-half was fixed in 0.5% PFA at room temperature for 1 hour and prepared as corneal flat-mounts. The other half was fixed in 2.5% glutaraldehyde at 4°C overnight and prepared for SEM examination.

For corneal flat-mounts, incubation with anti-ZO-1 for IHC was conducted as described earlier. For SEM examination, corneas were dehydrated with a series of graded concentrations of ethanol and dried in a vacuum. Then the endothelial surfaces were coated with gold-palladium before observation under a scanning electron microscope (JEOL, Tokyo, Japan).

Data Analysis and Statistics

All experiment was independently repeated three times. Image J software (National Institutes of Health, Bethesda,

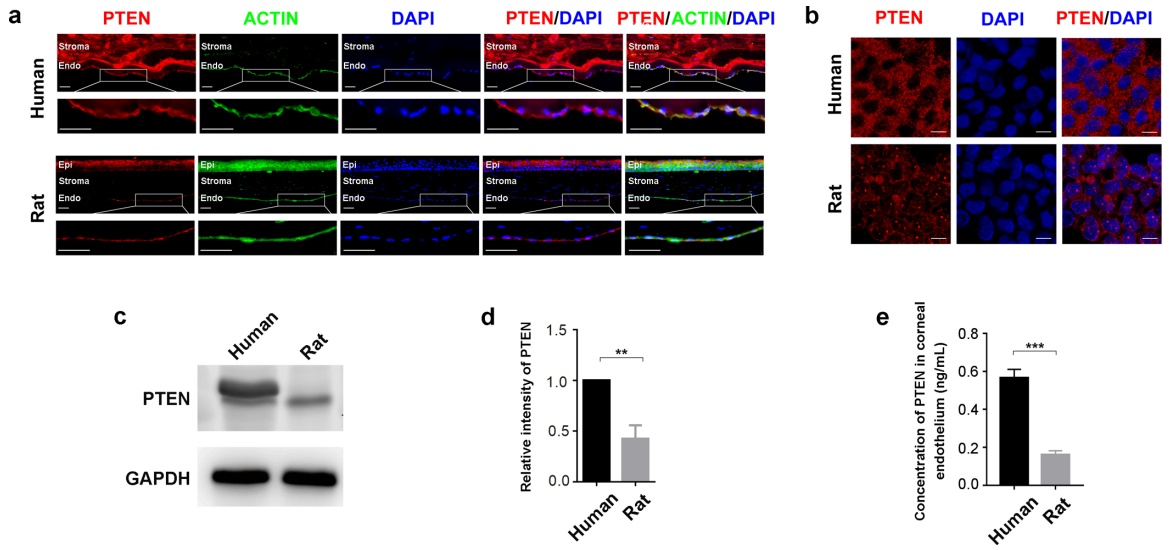

Figure 1. Differential expressions of PTEN in the human and rat corneal endothelium. (**a**) Immunofluorescence staining of PTEN (*red*) and actin detected by phalloidin antibody (*green*) in human and rat corneas. Cell nuclei were stained with DAPI (*blue*). *Scale bar* = 20 µm. $N = 3$. (**b**) Flat-mount staining of PTEN (*red*) in human and rat corneal endothelium. Cell nuclei were stained with DAPI (*blue*). *Scale bar* = 10 µm. $N = 3$. (**c, d**) Total protein was extracted from the corneal endothelium detached from human corneoscleral rims and rat corneas. Cell lysates were analyzed by western blotting and immunoblotted using an anti-PTEN antibody. Data are presented as the mean ± SD from three independent experiments and plotted as PTEN protein expression compared with the respective GAPDH control. $^{**}P < 0.01$ by the Student's *t*-test. (**e**) Total protein extracted from human ($N = 9$) and rat ($N = 6$) corneal endothelium tissue were analyzed by ELISA. Data are presented as the mean ± SD from three independent experiments and plotted as concentration of PTEN in the corneal endothelium (ng/mL). $^{***}P < 0.001$ by the Student's *t*-test.

MD, USA) was used to for gray scale analysis of the western blotting images, and intensity measurement of the immunofluorescent images.

To quantify the nuclear p27 fluorescence intensity, three to five separate microscopic fields from each group were randomly chosen, and 5 to 10 cells were counted for each field. The experiment was independently repeated three times. Cell nuclei were outlined according to DAPI staining (blue) with Image J software. The fluorescence intensity of p27 (red) in the nucleus profile was calculated as the fluorescence intensity value of p27 in cell nucleus. Then we got the quantified relative fluorescence intensity of p27 relative to the no-treatment control group (normalized to 1). During the entire process, the laser power, shooting parameters, and image processing were all consistent and conducted by dedicated technicians following the randomization and double-blinded principles.

Data are presented as the mean ± standard deviation (SD), with statistical significance assessed using the Student's *t*-test for comparison between the two groups, and 1-way ANOVA tests for multiple comparisons. A statistical test was performed using SPSS software (IBM Corp., Armonk, NY, USA) with $P<0.05$, which is considered as statistically significant.

Results

PTEN Expression in Corneal Endothelium was Higher in Humans Compared with Rats

First, PTEN expression was detected in human and rat corneal tissues by immunohistochemistry. As shown in Figure 1a, PTEN was detected in both human and rat corneas. Moreover, for CECs of the two species (Fig. 1b) PTEN expression was mainly found in the cytosol, and in rat CEC PTEN also seemed to localize to the nucleolus. Also, western blotting results (Figs. 1c, 1d) proved that the corneal endothelium tissue of humans had significantly higher PTEN expression compared with rats, as well as rabbits (see Supplementary Fig. S3). To further detect the concentration of PTEN in the corneal endothelium of the two species, we performed ELISA that showed that the concentration of PTEN in human CEC was 0.57 ± 0.04 ng/mL ($n = 9$), whereas the concentration in rat CEC was significantly different at 0.16 ± 0.02 ng/mL ($n = 6$) (Fig. 1e). Given the differences in the proliferative capacity between human and rat CECs, we speculated that the relatively high PTEN expression might be related to the phenomenon that human CECs tended to be more sensitive to TGF-β2.

PTEN Inhibition Led to Resistance to TGF-β2 Mediated G1-Arrest

To further explore the role of PTEN in TGF-β2-induced G1-arrest, we analyzed the cell cycle status of cultured B4G12 in the presence of TGF-β2, bpV(pic) (a small molecular PTEN inhibitor), or the combination of the two.

Flow cytometry results shown in Figures 2a and 2b illustrate that under basal conditions (control group), the percentages of cells in the G0/G1 and S phases were 67.48 ± 3.30% and 21.21 ± 0.43%, respectively. Treatment with 10 ng/mL of TGF-β2 for 24 hours (TGF-β2 group) caused a significant increase of cells in the G0/G1 phase (75.05% ± 1.40%) along with a marked decrease of cells in S phase (12.81% ± 1.17%), confirming that TGF-β2 led to G1-arrest in B4G12. In contrast, PTEN inhibition by treat-

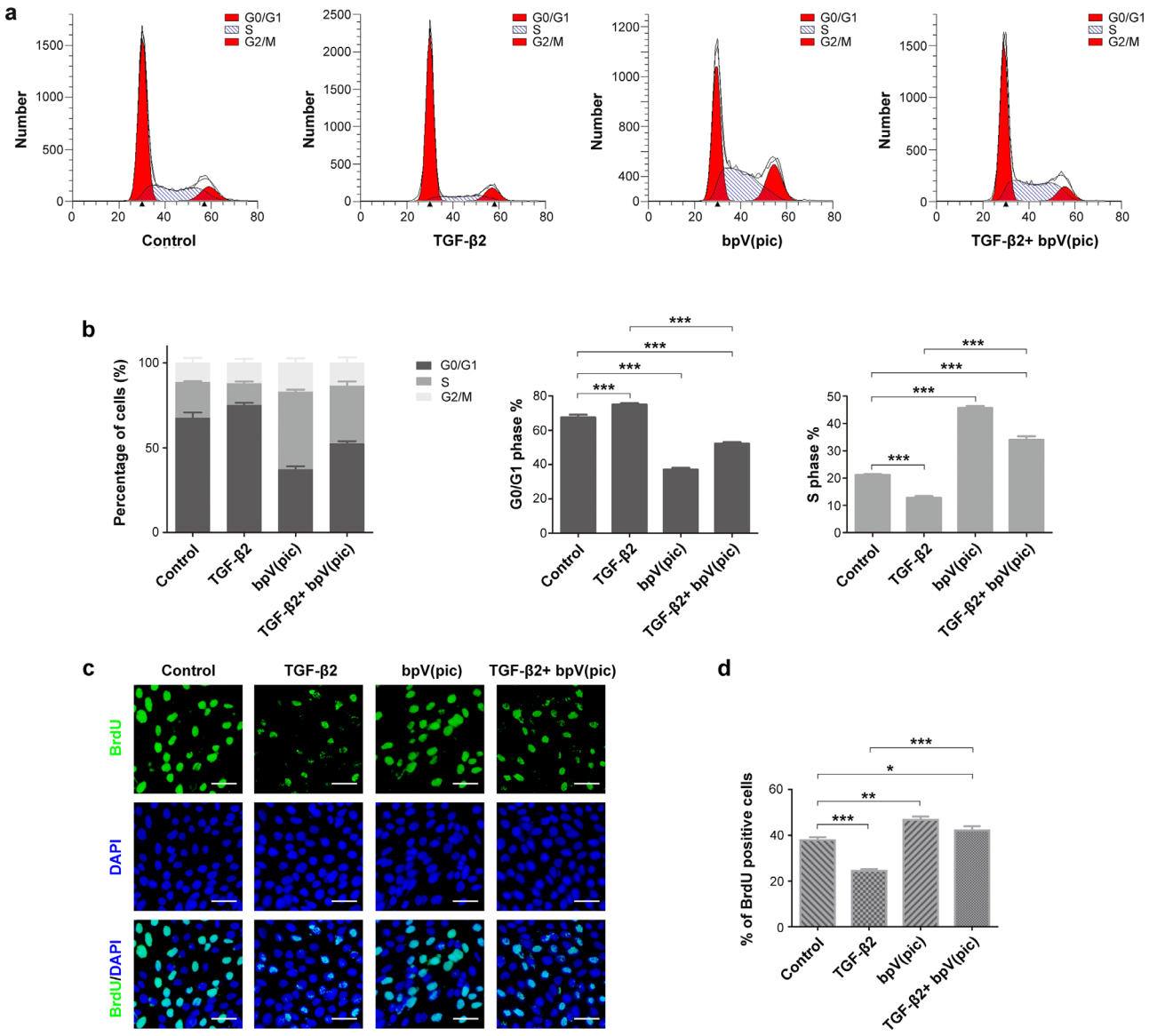

Figure 2. Inhibition of PTEN with bpV(pic) contributed to alleviate the TGF-β2-induced G1-arrest. Cell cycle synchronization of B4G12 cells was achieved by starvation in DMEM without FBS for 24 hours. B4G12 cells were then treated with 10 ng/mL TGF-β2, 10 µM bpV(pic), or the combination of the two supplemented in DMEM with 5% FBS. (**a**) After treatment for another 24 hours, cells were collected and underwent flow cytometry analysis. (**b**) Quantification data are presented as the mean ± SD from three independent experiments. $^{***}P <$ 0.001 by 1-way ANOVA. (**c**) BrdU immunofluorescence staining (*green*) was used to label S-phase cells after drug treatment (*blue* signals show nuclei counterstaining with DAPI). (**d**) The percentage of BrdU-positive cells are presented as the mean ± SD from three independent experiments. *Scale bar* = 50 µm. $^{*}P < 0.05$, $^{**}P < 0.01$, $^{***}P < 0.001$ by 1-way ANOVA.

ment with 10 µM bpV(pic) (bpV(pic) group) downregulated the percentage of cells in the G0/G1 phase to 37.12% ± 2.01%, and upregulated percentage of S-phase cells to 45.74% ± 1.34%, suggesting that PTEN inhibition promoted B4G12 cells to enter S phase. When TGF-β2 was applied together with 10 µM bpV(pic) (TGF-β2+bpV(pic) group), the percentage of cells in G0/G1 phase reached 52.29% ± 1.56%, and S phase reached 34.01% ± 2.72%, suggesting that TGF-β2-induced G1-arrest was attenuated. These findings support the idea that PTEN inhibition with bpV(pic) not only completely abolished the TGF-β2-mediated G1-arrest, but also facilitated CECs to further enter S phase. These results suggested that, rather than TGF-β2-mediated G1-arrest, other signaling pathways participate in regulating human CEC cell G1-arrest that can be regulated by PTEN.

BrdU is an analog of thymidine that is incorporated into newly synthesized DNA during S phase when DNA is replicated. When detected with anti-BrdU antibodies, only S-phase cells show positive staining, and so BrdU staining is a reliable and precise method to label replicating cells, which were released from G1-arrest status. The positive rates of BrdU staining at baseline, after treatment with TGF-β2, bpV(pic) and the combination of the two were 37.94% ± 1.06%, 24.47% ± 0.61%, 46.83% ± 1.12%, and 42.21% ± 1.50%, respectively (Figs. 2c, 2d). The results also proved that bpV(pic) rescued TGF-β2-mediated G1-arrest and further promoted more cells to enter S phase.

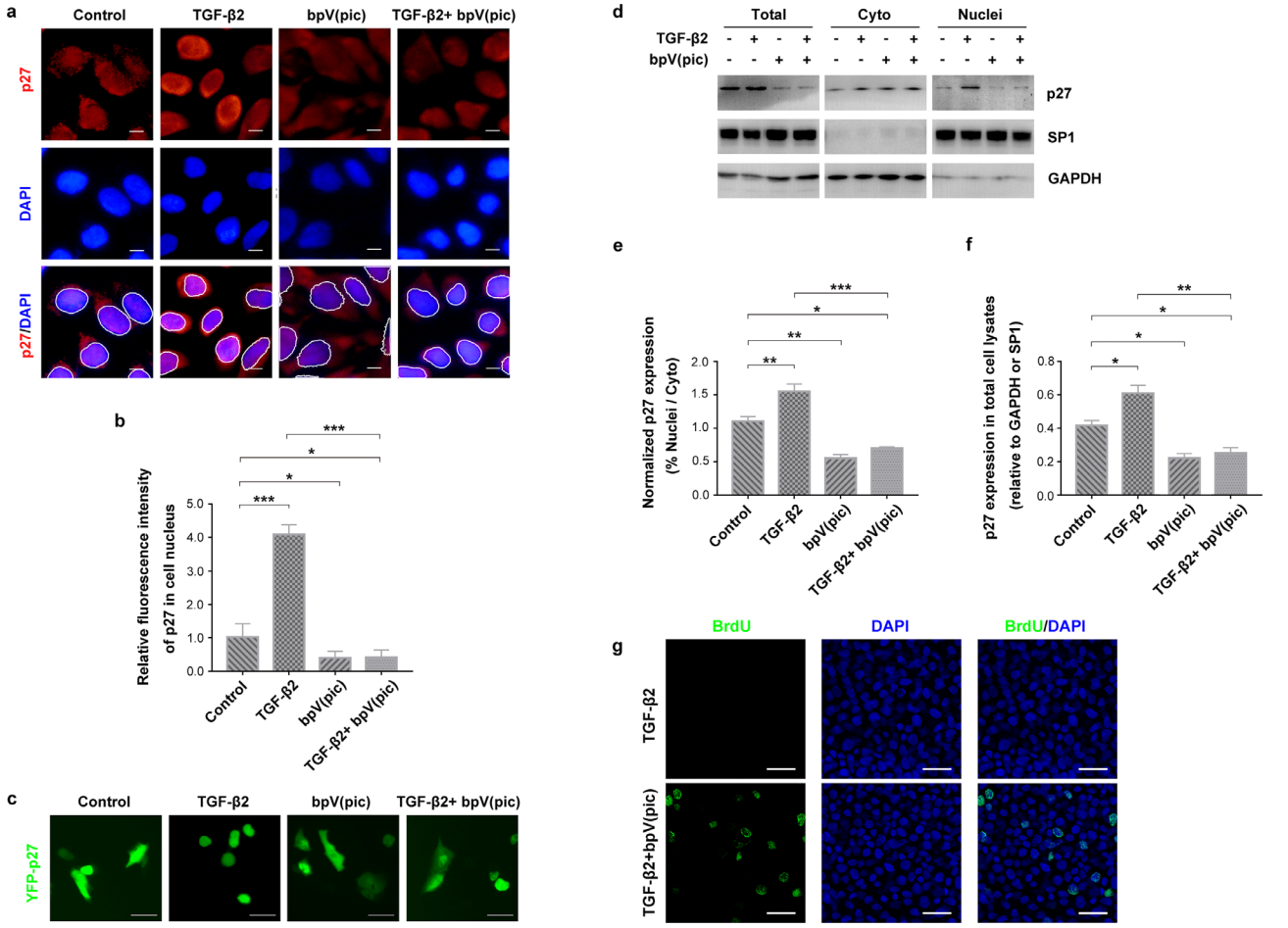

Figure 3. BpV(pic) facilitated p27 translocation to the cytoplasm and downregulated total p27 expression to relieve TGF-β2-induced p27 nuclear aggregation and promoted CECs entering S phase in organ-cultured rat corneas. (**a**) After treatment with 10 ng/mL TGF-β2, 10 µM bpV(pic), or the combination of the two for 24 hours, B4G12 cells were fixed and p27 immunofluorescence staining (*red*) was performed to visualize the endogenous p27 cellular location (*blue* signals show nuclei counterstaining with DAPI). *Scale bar* = 10 µm. (**b**) The fluorescence intensity of p27 in the nucleus from three independent experiments was normalized to that of the control group and expressed as the fold increase. $^{*}P < 0.05$, $^{***}P < 0.001$ by 1-way ANOVA. (**c**) B4G12 cells were transfected with the YFP-p27 plasmid and treated with 10 ng/mL TGF-β2, 10 µM bpV(pic), or the combination of the two for 24 hours. The cellular localization of transfected YFP-p27 was observed by direct fluorescence microscopy. *Scale bar* = 25 µm. (**d**) After drug treatment, the cytosolic (cyto) and nuclear fractions (nuclei), as well as whole cell lysates (total) of B4G12 were collected, and endogenous p27 levels in each fractionated extract were determined by immunoblotting. SP1 and GAPDH were used as nuclear and cytoplasmic loading controls, respectively. (**e**) Normalized p27 in the nuclear and cytosolic fractions were plotted as the ratio of nuclei to cytoplasm. $^{*}P < 0.05$, $^{**}P < 0.01$, $^{***}P < 0.001$ by 1-way ANOVA. $N = 3$. (**f**) The p27 expressions in the total cell lysate were normalized to relative loading controls. $^{*}P < 0.05$, $^{**}P < 0.01$ by 1-way ANOVA. $N = 3$. (**g**) Rat corneas were organ-cultured in Opti-MEM I media supplemented with 10 ng/mL TGF-β2, with or without 1µM bpV(pic) for 24 hours. BrdU immunofluorescence staining (*green*) was used to detect CEC in S phase (*blue* signals show nuclei counterstaining with DAPI). *Scale bar* = 10 µm.

PTEN Participated in TGF-β2-Induced G1-Arrest by Reducing the Nuclear p27Kip1 Accumulation

P27Kip1 is a cyclin-dependent kinase (CDK) inhibitor that is known to negatively regulate the kinase activities of the cyclinE/CDK2 and cyclinD/CDK4 complexes, thus facilitating S-phase entry and cell cycle progression.[25,26] We next investigated whether PTEN participated in TGF-β2-induced G1-arrest by regulating p27Kip1 nuclear accumulation in response to TGF-β2.

IHC results showed that endogenous p27Kip1 in B4G12 was uniformly distributed in the cytoplasm and nucleus in the control group (Figs. 3a, 3b). TGF-β2 treatment resulted in redistribution of p27Kip1 from the cytoplasm to nucleus in some cells, indicating G1-arrest was caused by TGF-β2. Moreover, PTEN inhibition by bpV(pic) treatment attenuated p27Kip1 nuclear accumulation induced by TGF-β2. The bpV(pic) treatment alone caused p27Kip1 distribution in cytoplasm and nucleus at more comparable levels to the control group.

To further highlight the translocation of p27Kip1, we transiently transfected fluorescent-tagged p27Kip1 (YFP-p27Kip1) into B4G12 cells, and exogenous p27Kip1 localization was directly observed under a fluorescent microscope. Our results showed that YFP-p27Kip1 was exclusively nuclear in response to TGF-β2 treatment, which was reversed by PTEN inhibition using bpV(pic) (Fig. 3c).

We separated nuclear and cytoplasmic fractions, and detected the expression of p27Kip1 by western blotting (Fig. 3d). Results indicated that TGF-β2 induced an apparent increase in the p27Kip1 nuclear-cytoplasmic ratio compared with the control group (Fig. 3e), along with an

increase of p27Kip1 expression in the total cellular lysate (Fig. 3f). These observations are consistent with previous studies: TGF-β2 led to CEC G1-arrest through induction of p27Kip1 nuclear accumulation, which hampered degradation of p27Kip1 in the cytoplasm via ubiquitination.[27] Taken together, PTEN inhibition abolished TGF-β2-induced p27Kip1 nuclear accumulation (Fig. 3e) and rescued the increase of total p27Kip1 expression (Fig. 3f). These effects further contributed to the nuclear export of p27Kip1 and decreased total p27Kip1 expression (Figs. 3e, 3f). It is also worth noting that PTEN inhibition with bpV(pic) treatment decreased the p27Kip1 nuclear-cytoplasmic ratio (Fig. 3e) and p27Kip1 expression in the total cellular lysate (Fig. 3f) compared with the control group, suggesting that p27Kip1 is the critical downstream regulator in the PTEN-regulated CEC cell cycle. These results may explain why PTEN inhibition could completely abolish TGF-β2-induced G1-arrest, and even promoted the observed G1-S-phase transition as shown in Figure 2.

We also preliminary explored how bpV(pic) regulated the TGF-β2-induced p27Kip1 nuclear accumulation (see Supplementary Fig. S4). For YFP-p27 fluorescence imaging, bpV(pic) inhibited the TGF-β2-induced nuclear-accumulation of p27, whereas LY294002 conversely antagonized the effect of bpV(pic) on the resistance of TGF-β2, suggesting that bpV(pic) functions via PI3K/Akt signaling pathway to regulate the TGF-β2 signaling (see Supplementary Fig. S4).

We also conducted flowcytometry, BrdU staining, and YFP-p27 fluorescence imaging with another PTEN inhibitor, VO-Ohpic (Sigma-Aldrich, St. Louis, MO, USA) (see Supplementary Fig. S5). Results also proved that inhibition of PTEN facilitated resistance of CECs to the TGF-β2-induced G1-arrest and promoted cell cycle progress.

Inhibition of PTEN Activity Released Rat CECs from G1-Arrest Status in the Organ-Cultured Cornea

We have shown that PTEN inhibition facilitates CECs to resist TGF-β2-induced G1-arrest in vitro. To further explore the feasibility of developing bpV(pic) as a small molecule inhibitor of PTEN that could be used to treat corneal endothelial dysfunction, we first tested whether bpV(pic) could be applied to an organ-cultured rat cornea system in vivo.

Complete corneas from rats were obtained and placed with the endothelium faced up in Opti-MEM I media supplemented with TGF-β2, or the combination of TGF-β2 and bpV(pic) and cultured for 24 hours. BrdU staining showed that when cultured with TGF-β2, the CECs of the rat cornea exhibited very weak BrdU staining. However, when supplemented with bpV(pic), some of the CECs exhibited positive BrdU staining, suggesting that these cells had entered S phase and started to proliferate, which was in agreement with the in vitro results (Fig. 3g).

Inhibition of PTEN Promoted CEC Migration by Activation of the PI3K/Akt Pathway

It is known that TGF-β2 promotes CEC migration through activation of P38 mitogen-activated protein kinases (MAPK) and PI3Ks signaling pathways.[28,29] Previous reports have demonstrated that downregulation of PTEN at the corneal epithelial wound edges facilitated the migration of peripheral corneal epithelial cells by increased Akt activation to significantly enhance the wound healing rate of corneal epithelial injury.[20,30] Considering the enhanced effect on cell migration, we aimed to explore if PTEN inhibition acted to synergize with the effects with TGF-β2 on CEC migration.

The migration of B4G12 cells was determined when treated with TGF-β2, bpV(pic), and in combination in vitro using a wound scratch model (Fig. 4a). Both TGF-β2 and bpV(pic) alone significantly increased the migration of B4G12 cells. Moreover, the enhanced effect of TGF-β2 on cell migration was further strengthened by bpV(pic) treatment, and this synergistic effect was completely abolished by LY294002, an inhibitor of the PI3K/Akt signaling pathway.

We also performed a transwell invasion assay to study the migratory response of B4G12 cells to the cytokines and inhibitors described earlier (Fig. 4b). The results were consistent with the migration assay conducted on the scratch model. PTEN inhibition with bpV(pic) further improved the motility of B4G12 cells compared with TGF-β2 treatment alone. LY294002 was shown to abrogate the promotion effect of their combination on cell motility.

In summary, these results demonstrated that PTEN inhibition assisted TGF-β2 by promoting migration of CECs through activation of the PI3K/Akt pathway.

Intracameral Injection of bpV(pic) Facilitated Corneal Endothelial Wound Healing in a Rat Corneal Endothelial Damage Model

Inhibition of PTEN with bpV(pic) released CECs from TGF-β2-induced G1-arrest status and promoted replication. Also, bpV(pic) had a synergistic role with TGF-β2 by increasing CEC migration. To further investigate the effect of PTEN inhibition on corneal endothelial wound healing in vivo, we employed a rat model induced by intracameral injection of 0.05% benzalkonium chloride.

Slit lamp biomicroscopy results demonstrated that at day 0, the corneal edema grading score was not significantly different between the two groups. PTEN inhibition by intracameral injection of bpV(pic) resulted in a significant reduction in the corneal edema grading score (Figs. 5a, 5b) at 7 and 14 days after operation compared with the control group, members of which were intracamerally injected with Opti-MEM I media (the solvent for bpV(pic)). These results indicated that PTEN inhibition promoted corneal transparency recovery.

We also measured the central corneal thickness (CCT) to quantitatively evaluate corneal edema regression. At 7 days after the operation, the CCT value of the bpV(pic) group (367.67 ± 33.76 µm) was significantly smaller than that of the control group (476.67 ± 24.63 µm) (Figs. 5c, 5d). At 14 days after the operation, the CCT in the control group decreased to 263.50 ± 19.34, and in the bpV(pic) group decreased to 160.17 ± 5.98, and significant difference in CCT between the two groups was still found. These data suggested that intracameral injection of bpV(pic) promoted the regression of corneal edema.

In addition, we performed histological and SEM examinations to observe the healing process of corneal endothelium in each group. ZO-1 is a tight junction-associated protein that can be used to evaluate the integrity of the corneal endothelium barrier. IHC staining showed that

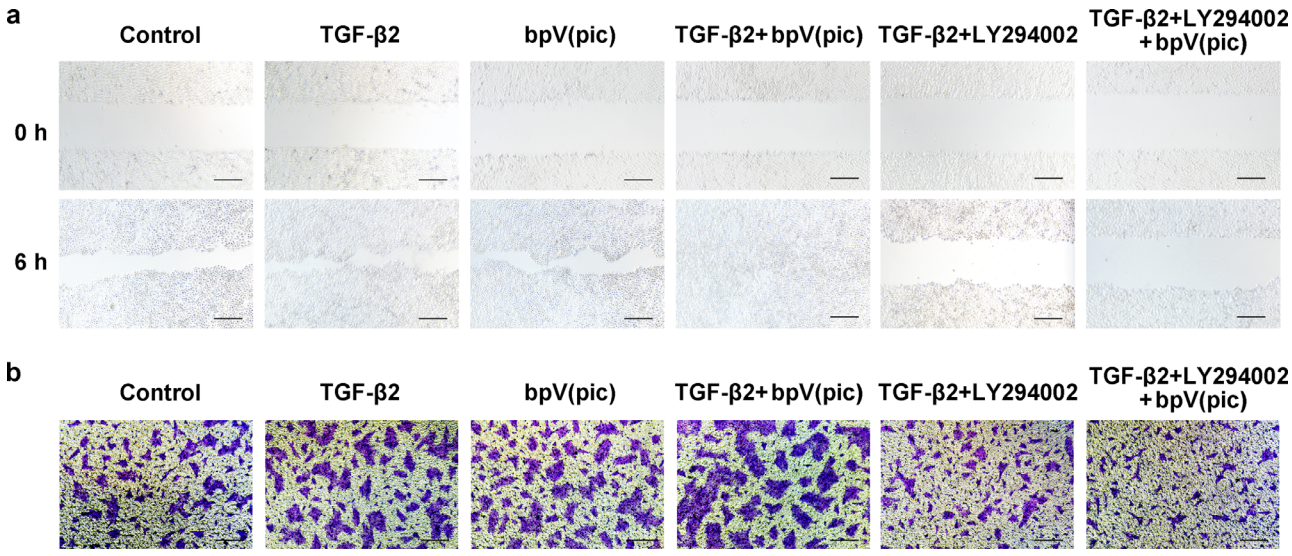

Figure 4. Inhibition of PTEN with bpV(pic) enhanced the promotion effect of TGF-β2 on CEC migration through activating the PI3K/Akt signaling pathway. (**a**) A scratch on the confluent B4G12 monolayer was made, followed by treatment with different drugs. Wound healing was recorded during the next 6 hours. *Scale bar* = 100 µm. $N = 3$. (**b**) Cell invasion assay was conducted and after drug treatment for 12 hours, the migrating cells were visualized through crystal violet staining. *Scale bar* = 100 µm. $N = 3$.

normal corneal endothelium exhibited contiguous ZO-1 expression at the cell-cell borders (Fig. 5e). Immediately after the intracameral injection of 0.05% benzalkonium chloride, which induced corneal endothelial injury (day 0), the expression of ZO-1 significantly decreased, indicating the destruction of the barrier integrity. During the subsequent wound healing process of the corneal endothelium, the bpV(pic) group showed an apparently higher cell density comparing to the control group with better re-establishment of barrier function at 7 and 14 days after the operation.

SEM examinations were conducted to visualize the healing process of the corneal endothelium (Fig. 5f). A delicate monolayer composed of closely linked hexagonal CECs could be seen at the inner face of the normal cornea. Benzalkonium chloride induced apparent endothelial cellular edema, as well as destruction of intercellular tight junctions at day 0. The CECs that were hydropically degenerated were then detached form the Descemet membrane, leaving a large area of denuded zone without coverage of CECs. During the healing process, peripheral CECs proliferate and migrate to cover the denuded basement membrane. At 7 days after the operation, the corneal endothelium in the bpV(pic) group had formed an intact monolayer with established intercellular junctions and some edematous CECs remained. In the control group, denuded areas with no CEC coverage could still be seen. At 14 days after operation, the CEC monolayer in the bpV(pic) group had almost recovered showing normal structure and morphology. In contrast, CECs in the control group still exhibited an edematous appearance, although no denuded zone could be seen, with no established intercellular junctions observed.

Based on these experimental findings, we proposed a model for PTEN in the regulation of corneal endothelial wound healing (Fig. 6). PTEN inhibition with bpV(pic) abolished TGF-β2-induced G1-arrest and facilitated cell migration of CECs through a pathway that involved p27Kip1 and the PI3K/Akt signaling pathway. The enhanced cell proliferation and migration jointly promoted corneal endothelium regeneration in situ.

To conclude, our results demonstrate that intracameral injection of bpV(pic) could improve CEC proliferation and migration and promote the re-establishment of a functional corneal endothelium to facilitate corneal endothelial wound healing.

Discussion

Here, to our knowledge, for the first time we demonstrated that the PTEN inhibitor, bpV(pic), could release CECs from a G1-arrested state mediated by TGF-β2, and thus promote cell cycle progression. Moreover, bpV(pic) promoted CEC migration in synergy with TGF-β2. Intracameral injection of bpV(pic) in a rat corneal endothelial injury model accelerated the wound healing process and may therefore provide therapeutic benefit for the regression of corneal edema and recovery of corneal transparency.

Human CECs are arrested in the G1-phase in vivo due to contact inhibition or high concentrations of TGF-β2 in the aqueous humor.[5] CECs may be injured by various etiologies, including aging, trauma, inflammatory disease, and corneal endothelial dystrophy. Once injured, CECs rarely divide, and when the cell density decreases to a critical level, residual CECs can no longer maintain a barrier and sufficient pump function to counteract swelling pressure, and so corneal endothelial dysfunction occurs.[5] The retention of sufficient CEC density is therefore critical to the health of the corneal endothelium. Accordingly, to explore factors that mediate the release of CECs from G-phase arrest may be critically important to the regeneration of corneal endothelium in situ during wound healing. During maturation of the corneal endothelium, the G1-arrest state was induced by increasingly stronger cell-cell contact inhibition. Once the intact corneal endothelial monolayer is established, maintenance of the G1-arrest is mainly mediated by TGF-β2.[31,32] Moreover, elevated levels of active TGF-β2 in the aqueous

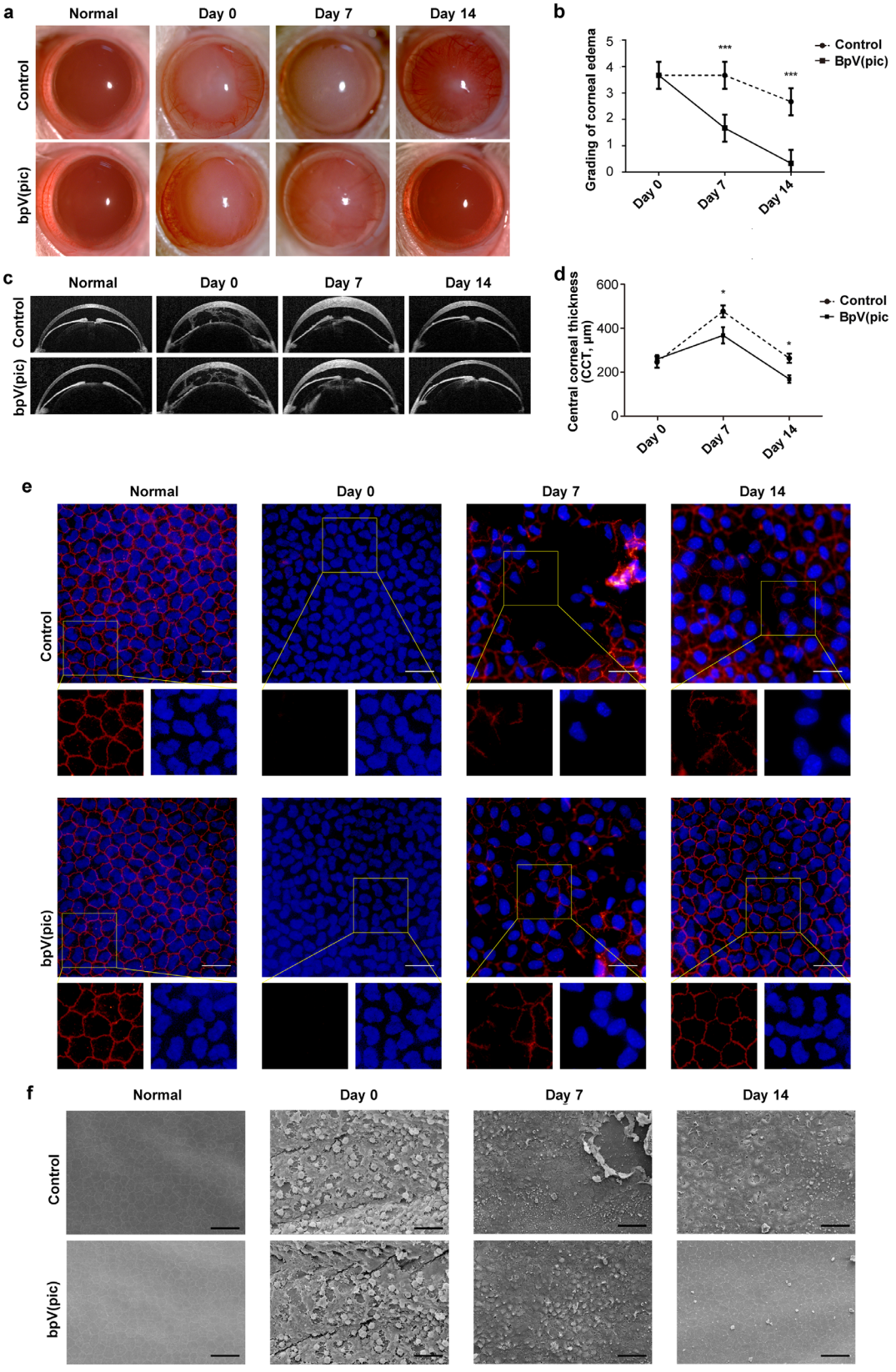

Figure 5. Intracameral injection of bpV(pic) promoted corneal transparency recovery, edema regression, as well as histological and morphologic recovery in a rat corneal endothelial damage model. Rat corneal endothelial injury models were established and intracamerally injected with 5 μL Opti-MEM I (control group, $N = 12$) and 10 μM bpV(pic) diluted in 5 μL Opti-MEM I (bpV(pic) group, $N = 12$). (**a**) Representative photographs of members of each group during a 2-week follow-up period recorded with slit-lamp biomicroscopy. (**b**) Corneal edema grading scores were evaluated three times independently and presented as the mean ± SD. $^{***}P < 0.01$ by 1-way ANOVA. $N = 12$ for normal and at

day 0. $N = 10$ at day 7. $N = 8$ at day 14. (**c**) Anterior segment OCT images taken at each point during the follow-up. (**d**) CCT was measured and presented as the mean ± SD. $^{*}P < 0.05$ by 1-way ANOVA. $N = 12$ for normal and at day 0. $N = 10$ at day 7. $N = 8$ at day 14. (**e**) Corneas of each group were fixed and stained by immunofluorescence for ZO-1 (*red*) and DAPI (*blue*) to show cell barrier formation, as well as cell density at the indicated time points. *Scale bar* = 25 µm. $N = 4$ at each time point. (**f**) SEM of corneas at the indicated time points exhibited the exact morphologic changes during the wound healing process. *Scale bar* = 50 µm. $N = 3$ at each time point.

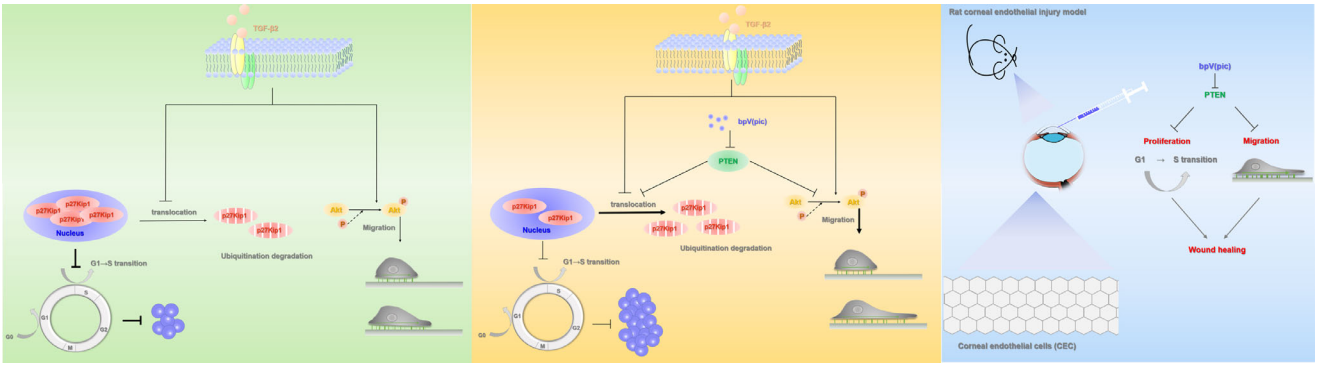

Figure 6. A model for the mechanism of PTEN regulating corneal endothelial wound healing. PTEN inhibition with bpV(pic) released CECs from TGF-β2-induced G1-arrest and promoted CEC migration in synergy with TGF-β2 through regulating p27Kip1 and PI3K/Akt pathway, thus improved corneal endothelial regeneration in situ in a rat corneal endothelial injury model.

humor were detected during the aging process,[33] and in patients with posterior polymorphous corneal dystrophy.[34] Considering the occurrence of corneal endothelial dysfunction mainly in adulthood, investigation into the mechanism of CEC proliferation under the effects of TGF-β2 is of significance and may facilitate the development of new therapies.

Our results showed that inhibition of PTEN with bpV(pic) completely abolished TGF-β2-induced G1-arrest in human CECs, by relieving the TGF-β2-mediated p27Kip1 nuclear accumulation and increase of total expression (Figs. 2, 3). Compared with the control group, bpV(pic) further promoted S-phase entry of CECs (Fig. 2). These data suggested that PTEN alone could affect CEC S-phase entry. Further studies showed that PTEN inhibition promoted G1-S transition by facilitating p27Kip1 nuclear export and degradation in the cytoplasm (Fig. 3).

The wound healing process of the corneal endothelium, particularly in primates and feline, has an important peculiarity in that it is mainly completed by cell migration and enlargement of adjacent healthy cells and rarely involves proliferation.[5] We also explored the role of PTEN in cell migration. TGF-β2 has been reported to promote CEC migration by activating the P38 MAPK and PI3Ks signaling pathways.[28,29] In our study, enhanced migration of CECs was observed in response to TGF-β2, which could be completely blocked by LY294002, an inhibitor of PI3K/Akt (Fig 4). Meanwhile, inhibition of PTEN by bpV(pic) also accelerated CEC migration. When applied together, synergistic effects between TGF-β2 and bpV(pic) on cell migration were observed, which could also be blocked by LY294002. PTEN has been reported to direct the migration of corneal epithelial cells to wounded areas.[30] Furthermore, PTEN inhibition by bpV(pic) could accelerate corneal epithelial wound healing cell migration through activation of Akt[20] signaling, which is consistent with our results (Fig. 4).

The CECs of primates and feline cannot enter S-phase when injured, whereas the CECs of rabbits and rats can be released from G1-arrest status and start to divide.[5,8,9] These data indicated that the sensitivity of CECs to TGF-β2-induced G1-arrest is species-specific, and this may also explain differential proliferation capacities when cultured in vitro. We demonstrated that PTEN is expressed at a relatively higher level in the corneal endothelium of human compared with rats (Fig. 1). It is well known that PTEN downregulates the Akt signaling pathway and acts as a tumor suppressor by regulating cell cycle and proliferation.[14–16] PTEN mutation or deletion occurs in several human tumors and is accompanied with aggressive activation of Akt signaling.[35,36] In addition, various factors, including FGF-2,[37–39] IGF-1,[40] Y-27632,[41] and mesenchymal stem cell–derived conditioned medium,[42] have been reported to promote CEC proliferation by activating the PI3K/Akt signaling pathway. Moreover, it was reported that cells with higher pAkt levels are more resistant to TGF-β2-induced G1-arrest.[30] Therefore we speculated that species differences in the cell cycle of CECs in response to TGF-β2 once injured and the proliferative capacity in vitro might be due to intrinsic differences of PTEN expression. The bpV(pic) could have potential for a treatment of corneal endothelial dysfunction. Meanwhile, the subcellular location of PTEN seemed to be different in human and rat CEC (Fig. 1b). As reported, the definite subcellular locations of PTEN performed distinct biological functions.[43] For instance, PTEN located on endoplasmic reticulum and mitochondrial-associated membranes mainly play the role of lipid phosphatase activity to inhibit PI3K/AKT pathway. Further studies focusing on the PTEN subcellular location in the regulation of CEC cell cycle will guide the development of novel therapies.

We simulated in vivo conditions and applied bpV(pic) to an organ-cultured rat cornea. The result confirmed an S-phase transition promotion effect of bpV(pic) in the presence of TGF-β2 (Fig. 3g). In a rat corneal endothelial injury model induced by intracameral injection of benzalkonium chloride, we found that bpV(pic) could enhance the G1-S transition and the migration of CECs in the presence of TGF-β2. The observed dual function accelerated

wound healing in the rat corneal endothelium and is beneficial for the regression of corneal edema and recovery of corneal transparency. This was confirmed by slit lamp biomicroscopy and OCT (Fig. 5a–d). According to the IHC and SEM results, intracameral injection of benzalkonium chloride first disrupted the cell barriers (Fig. 5e at day 0), leading to CEC swelling and partially detaching from the Descemet membrane (Fig. 5f at day 0). During the healing process, PTEN inhibitor promoted the proliferation and migration of the remaining healthy CECs, and thus facilitated better recovery of cell density, as well as barrier function (Figs. 5e, 5f). These results suggest that PTEN could be a potential therapeutic target in the treatment of corneal endothelial dysfunction.

So far, we have demonstrated the positive effect of PTEN in relieving TGF-β2-mediated G1-arrest in CECs. Further exploration of the role of PTEN in the regulation of cell cycle arrest induced by contact inhibition in CECs should be undertaken.

Conclusions

In this study, we provided evidence to support PTEN inhibition by bpV(pic) in releasing CECs from G1-phase arrest induced by TGF-β2. These effects are mediated by p27 nuclear export and subsequent degradation in the cytoplasm. What is more, PTEN inhibition also promotes CEC migration in synergy with TGF-β2 through activation of the Akt signaling pathway. Intracameral injection of bpV(pic) therefore facilitates the regeneration of corneal endothelium in situ, and PTEN may have potential as a therapeutic target in corneal endothelial dysfunction.

Acknowledgments

Supported by the National Natural Science Foundation (81770888, 81800873, 31800809, 31500835), the Shanghai Municipal Education Commission-Gaofeng Clinical Medicine Grant Support (20161421), the Science and Technology Commission of Shanghai Grant (17DZ2260100, 17411963800, 19JC1411703), the Shanghai Pujiang Program (18PJD025) and the Shanghai Jiao Tong University School of Medicine Two-hundred Talent (20191914).

Disclosure: **W. Zhang,** None; **F. Yu,** None; **C. Yan,** None; **C. Shao,** None; **P. Gu,** None; **Y. Fu,** None; **H. Sun,** None; **X. Fan,** None

References

1. Gain P, Jullienne R, He Z, et al. Global survey of corneal transplantation and eye banking. *JAMA Ophthalmol*. 2016;134:167–173.
2. Price MO, Price FW, Jr. Endothelial keratoplasty–a review. *Clin Exp Ophthalmol*. 2010;38:128–140.
3. Joyce NC, Meklir B, Joyce SJ, Zieske JD. Cell cycle protein expression and proliferative status in human corneal cells. *Invest Ophthalmol Vis Sci*. 1996;37:645–655.
4. Engelmann K, Bohnke M, Friedl P. Isolation and long-term cultivation of human corneal endothelial cells. *Invest Ophthalmol Vis Sci*. 1988;29:1656–1662.
5. Joyce NC. Proliferative capacity of corneal endothelial cells. *Exp Eye Res*. 2012;95:16–23.
6. Joyce NC. Proliferative capacity of the corneal endothelium. *Prog Retin Eye Res*. 2003;22:359–389.
7. Joyce NC. Cell cycle status in human corneal endothelium. *Exp Eye Res*. 2005;81:629–638.
8. Joyce NC, Navon SE, Roy S, Zieske JD. Expression of cell cycle-associated proteins in human and rabbit corneal endothelium in situ. *Invest Ophthalmol Vis Sci*. 1996;37:1566–1575.
9. Van Horn DL, Sendele DD, Seideman S, Buco PJ. Regenerative capacity of the corneal endothelium in rabbit and cat. *Invest Ophthalmol Vis Sci*. 1977;16:597–613.
10. Capella JA. Regeneration of endothelium in diseased and injured corneas. *Am J Ophthalmol*. 1972;74:810–817.
11. Savion N, Isaacs JD, Shuman MA, Gospodarowicz D. Proliferation and differentiation of bovine corneal endothelial cells in culture. *Metab Pediatr Syst Ophthalmol*. 1982;6:305–320.
12. Waring GO, 3rd, Bourne WM, Edelhauser HF, Kenyon KR. The corneal endothelium. Normal and pathologic structure and function. *Ophthalmology*. 1982;89:531–590.
13. Pistsov MY, Sadovnikova E, Danilov SM. Human corneal endothelial cells: isolation, characterization and long-term cultivation. *Exp Eye Res*. 1988;47:403–414.
14. Li DM, Sun H. PTEN/MMAC1/TEP1 suppresses the tumorigenicity and induces G1 cell cycle arrest in human glioblastoma cells. *Proc Natl Acad Sci U S A*. 1998;95:15406–15411.
15. Xu W, Yang Z, Xie C, et al. PTEN lipid phosphatase inactivation links the hippo and PI3K/Akt pathways to induce gastric tumorigenesis. *J Exp Clin Cancer Res*. 2018;37:198.
16. Malek M, Kielkowska A, Chessa T, et al. PTEN regulates PI(3,4)P2 signaling downstream of class I PI3K. *Mol Cell*. 2017;68:566–580.e10.
17. Brandmaier A, Hou S-Q, Shen WH. Cell cycle control by PTEN. *J Mol Biol*. 2017;429:2265–2277.
18. Samarakoon R, Helo S, Dobberfuhl AD, et al. Loss of tumour suppressor PTEN expression in renal injury initiates SMAD3- and p53-dependent fibrotic responses. *J Pathol*. 2015;236:421–432.
19. Zhao M, Song B, Pu J, et al. Electrical signals control wound healing through phosphatidylinositol-3-OH kinase-gamma and PTEN. *Nature*. 2006;442:457–460.
20. Cao L, Graue-Hernandez EO, Tran V, et al. Downregulation of PTEN at corneal wound sites accelerates wound healing through increased cell migration. *Invest Ophthalmol Vis Sci*. 2011;52:2272–2278.
21. Eveleth DD, Eveleth JJ, Subramaniam A, et al. An engineered human fibroblast growth factor-1 derivative, TTHX1114, ameliorates short-term corneal nitrogen mustard injury in rabbit organ cultures. *Invest Ophthalmol Vis Sci*. 2018;59:4720–4730.
22. Dhillon VK, Elalfy MS, Messina M, Al-Aqaba M, Dua HS. Survival of corneal nerve/sheath structures in organ-cultured donor corneas. *Acta Ophthalmol*. 2018;96:e334–e340.
23. Segarra S, Leiva M, Costa D, et al. A dose-escalation ex vivo study on the effects of intracameral benzalkonium chloride in rabbits. *BMC Vet Res*. 2018;14:39.
24. Hayashi T, Yamagami S, Tanaka K, et al. A mouse model of allogeneic corneal endothelial cell transplantation. *Cornea*. 2008;27:699–705.
25. Sutterluty H, Chatelain E, Marti A, et al. p45SKP2 promotes p27Kip1 degradation and induces S phase in quiescent cells. *Nat Cell Biol*. 1999;1:207–214.
26. von Harsdorf R, Hauck L, Mehrhof F, Wegenka U, Cardoso MC, Dietz R. E2F-1 overexpression in cardiomyocytes induces downregulation of p21CIP1 and p27KIP1 and release of active cyclin-dependent kinases in the presence of insulin-like growth factor I. *Circ Res*. 1999;85:128–136.
27. Kim TY, Kim WI, Smith RE, Kay ED. Role of p27(Kip1) in cAMP- and TGF-beta2-mediated antiproliferation in rabbit corneal endothelial cells. *Invest Ophthalmol Vis Sci*. 2001;42:3142–3149.

Investigative Ophthalmology & Visual Science

28. Joko T, Shiraishi A, Kobayashi T, Ohashi Y, Higashiyama S. Mechanism of proliferation of cultured human corneal endothelial cells. *Cornea*. 2017;36(suppl 1):S41–S45.
29. Lee JG, Kay EP. Common and distinct pathways for cellular activities in FGF-2 signaling induced by IL-1beta in corneal endothelial cells. *Invest Ophthalmol Vis Sci*. 2009;50:2067–2076.
30. Liang J, Zubovitz J, Petrocelli T, et al. PKB/Akt phosphorylates p27, impairs nuclear import of p27 and opposes p27-mediated G1 arrest. *Nat Med*. 2002;8:1153–1160.
31. Joyce NC, Harris DL, Zieske JD. Mitotic inhibition of corneal endothelium in neonatal rats. *Invest Ophthalmol Vis Sci*. 1998;39:2572–2583.
32. Joyce NC, Harris DL, Mello DM. Mechanisms of mitotic inhibition in corneal endothelium: contact inhibition and TGF-beta2. *Invest Ophthalmol Vis Sci*. 2002;43:2152–2159.
33. Trivedi RH, Nutaitis M, Vroman D, Crosson CE. Influence of race and age on aqueous humor levels of transforming growth factor-beta 2 in glaucomatous and nonglaucomatous eyes. *J Ocul Pharmacol Ther*. 2011;27:477–480.
34. Stadnikova A, Dudakova L, Skalicka P, Valenta Z, Filipec M, Jirsova K. Active transforming growth factor-beta2 in the aqueous humor of posterior polymorphous corneal dystrophy patients. *PLoS One*. 2017;12:e0175509.
35. Kopp JL, Dubois CL, Schaeffer DF, et al. Loss of Pten and Activation of Kras Synergistically Induce Formation of Intraductal Papillary Mucinous Neoplasia From Pancreatic Ductal Cells in Mice. *Gastroenterology*. 2018;154:1509–1523.e1505.
36. Li X, Mak VCY, Zhou Y, et al. Deregulated Gab2 phosphorylation mediates aberrant AKT and STAT3 signaling upon PIK3R1 loss in ovarian cancer. *Nat Commun*. 2019;10:716.
37. Kay EP, Park SY, Ko MK, Lee SC. Fibroblast growth factor 2 uses PLC-gamma1 for cell proliferation and PI3-kinase for alteration of cell shape and cell proliferation in corneal endothelial cells. *Mol Vis*. 1998;4:22.
38. Lee HT, Kay EP. Regulatory role of cAMP on expression of Cdk4 and p27(Kip1) by inhibiting phosphatidylinositol 3-kinase in corneal endothelial cells. *Invest Ophthalmol Vis Sci*. 2003;44:3816–3825.
39. Lee JG, Song JS, Smith RE, Kay EP. Human corneal endothelial cells employ phosphorylation of p27(Kip1) at both Ser10 and Thr187 sites for FGF-2-mediated cell proliferation via PI 3-kinase. *Invest Ophthalmol Vis Sci*. 2011;52:8216–8223.
40. Sabater AL, Andreu EJ, Garcia-Guzman M, et al. Combined PI3K/Akt and Smad2 activation promotes corneal endothelial cell proliferation. *Invest Ophthalmol Vis Sci*. 2017;58:745–754.
41. Okumura N, Nakano S, Kay EP, et al. Involvement of cyclin D and p27 in cell proliferation mediated by ROCK inhibitors Y-27632 and Y-39983 during corneal endothelium wound healing. *Invest Ophthalmol Vis Sci*. 2014;55:318–329.
42. Nakahara M, Okumura N, Kay EP, et al. Corneal endothelial expansion promoted by human bone marrow mesenchymal stem cell-derived conditioned medium. *PLoS One* 2013;8:e69009.
43. Bononi A, Pinton P. Study of PTEN subcellular localization. *Methods*. 2015;77–78:92–103.

Investigative Ophthalmology & Visual Science